Seasonal Characteristics and Interannual Variability of Monthly Scale Low-Frequency Oscillation in a Low-Order Global Spectral Model

Ni Yunqi (倪允琪)
Department of Atmospheric Sciences, Nanjing University
Zhang Qin (张 勤)
Nanjing Institute of Meteorology
and *Lin Wuyin* (林武银)
Department of Atmospheric Sciences, Nanjing University
Received May 24, 1990; revised November 22, 1990

ABSTRACT

Analysis is done of five-year low-pass filtered data by a five-layer low-order global spectral model, indicating that although any non-seasonal external forcing is not considered in the model atmosphere, monthly-scale anomaly takes place which is of remarkable seasonality and interannual variability.

Analysis also shows that for the same seasonal external forcing the model atmosphere can exhibit two climatic states, similar in the departure pattern but opposite in sign, indicating that the anomaly is but the manifestation of the adverse states, which supports the theory of multi-equilibria proposed by Charney and Devore(1979) once again.

Finally, the source for the low-frequency oscillation of the global atmosphere is found to be the convective heat source / sink inside the tropical atmosphere as discussed before in our study.

Therefore, the key approach to the exploration of atmospheric steady low-frequency oscillation and the associated climatic effect lies in the examination of the distribution of convective heat sources / sinks and the variation in the tropical atmosphere.

I. INTRODUCTION

Based on the study of Northern winter teleconnections, Wallace and Gutzler (1981) pointed out five typical teleconnections such as the Pacific / Northern America (PNA), the western Pacific (WP), the eastern Atlantic (EA), the western Atlantic (WA) and the Eurasian (EUP). Their study has great significance to understanding the quasi-stationary structure of atmospheric circulations in the Northern winter and improving long-term weather prediction and short-term climate forecasting. The establishment of the theory on two dimensional Rossby wave travelling over the sphere (Hoskins and Karoly, 1981) makes possible further explanation of the existence of the teleconnections. Horel and Wallace (1981) showed that during the ENSO episode in the Northern winter the response of the atmosphere to the tropical heat source may cause a stationary wave train of equivalent barotropic structure travelling across the Pacific and North America. Since then, meteorologists have paid renewed attention to the exploration of the forced response of atmosphere to the anomaly of the tropical SST by theoretical models and GCM. Shukla and Wallace (1983), Geisler et al. (1985) and Ni et al. (1990) reported that two-dimensional wave train similar to the PNA is simulated in the Northern winter by exploring the response of the atmosphere to the anomaly of the tropical

SST by GCM. These studies indicated that the SST anomaly as an external forcing can result in the atmospheric anomaly analogous to some teleconnection.

Through analyses of 15-year simulations with GCM, Lau (1981) showed that anomaly may take place in the model atmosphere without any non-seasonal external forcing. Apparently, this is the result of dynamic processes inside the atmosphere. Charney and Devore (1979) have confirmed that multi-equilibria can exist in the ideal channel model under the condition of steady external forcing. Therefore, they believed that the atmospheric anomaly can be the manifestation of different equilibria for the given external forcing, and the monthly-scale atmospheric variation may result from the transition from one equilibrium to another.

The above studies show that the atmospheric anomaly is caused mainly by anomalous external forcing and dynamic processes inside the atmosphere. Hence further investigation of the variations of monthly-and seasonal-scale anomalies without nonseasonal external forcing is of much theoretical significance and useful applications to understanding the natural variability intrinsic in the atmosphere itself, to further appreciation of the possible climatic effect caused by the forcing, and improving long-term weather prediction and short-term climatic forecasting. Attempt is made to analyse the seasonality and interannual variability of the monthly-and seasonal-scale oscillation by 5-year data of low-order global spectral model in order to investigate the natural variability intrinsic in the model atmosphere itself and hence to make further study of the climatic effect due to the anomaly of the external forcing by GCM.

A brief description of the model used is given in Section II; Section III discusses the seasonal characteristics of the monthly-scale oscillation; Section IV is devoted to the interannual variability of the oscillation; Section V deals with the source for the monthly-scale oscillation, with the discussion and summary given in the last section.

II. THE BRIEF DESCRIPTION OF THE MODEL AND TREATMENT OF SIMULATED DATA

The model used is a five-layer low-order global spectral model, which uses σ coordinates in the vertical with five layers from top of the model atmosphere to surface involved, and triangular truncation in the horizontal with the truncated wavenumber of 10. The basic equation system consists of the vorticity equation, horizontal divergence equation, continuity equation giving surface pressure through integration, thermodynamic equation and moisture equation. The processes of physical parameterization in the model include long-and short-wave radiation, large scale condensation and cumulus convection, horizontal and vertical diffusion of momentum, heat and vapour, with the consideration of the effect of the underlying surface(including seas, polar ice cap, and snow-cover) and topography on the atmospheric model. The solution of the model is by way of the Galerkin method and by the semi-implicit scheme for time integration with step length of 90 minutes. The integration runs starting from the rest, isothermal and dry atmosphere for six and a half years. We use the last five-year integrations as the simulated data for diagnostic analysis.

We treat these data by the 21-point filter similar to the low-pass filtering of Blackmon (1976) in order to analyse the seasonality and interannual variability of the monthly-scale oscillation. The filter can be expressed as the following:

$$\tilde{x}(t_i) = a_0 x(t_i) + \sum_{p=1}^{10} a_p [x(t_i + p) + x(t_i - p)] \quad ,$$

where $x(t_i)$ is the non-filtered daily simulated data; $\tilde{x}(t_i)$ low-pass filtered data and the

coefficient a_p is given in Table 1. The filter reserves the disturbance of $10 \leqslant T \leqslant 90$ days. All analyses presented are based on the low-pass filtered data.

Table 1. 21-Point Low-Pass Filtering Coefficients a_p and Their Values

Coefficient	Value
a_0	0.2119623984
a_1	0.1974416342
a_2	0.1576890490
a_3	0.1028784073
a_4	0.0462514755
a_5	0.0
a_6	−0.0281981813
a_7	−0.0368362395
a_8	−0.0300256308
a_9	−0.0151817136
a_{10}	0.0

III. SEASONAL CHARACTERISTICS OF MONTHLY-SCALE LOW-FREQUENCY OSCILLATION

Figs. 1a–d show the spatial distribution of the first principal components obtained by expanding EOF of 300 hPa geopotential height fields, averaged over 15 spring, summer, autumn and winter months, separately.

Comparing Figs. 1a–d , we can see that EOF1 is the strongest (weakest), in the winter (summer) hemisphere, with the other seasons in between. We can see from Fig. 1b that EOF1 is very weak in the pattern of the Northern summer, while in the SH there is a pattern of a positive alternating with a negative centre very similar to a wave train. The distribution of EOF1 in the northern autumn is given in Fig.1c, from which one can see the remarkable intensification (weakening) of EOF1 in the NH (SH). In the NH are seen two patterns analogous to wave trains of alternating positive and negative centres. One originating in the equatorial western Pacific moves towards the north, turns to the southeast in the North Pacific,

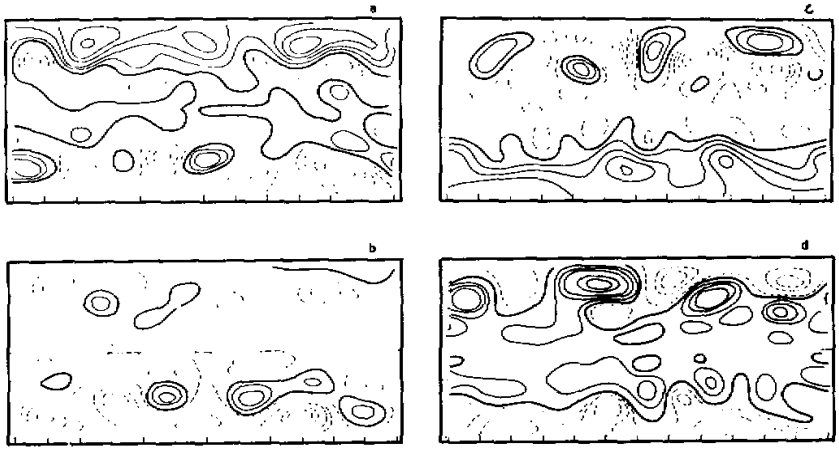

Fig.1. Spatial distribution of EOF1 of the 300 hPa geopotential height. a) Spring (March–May); b) Summer (June–August); c) Autumn (September–November); d) Winter (December–February).

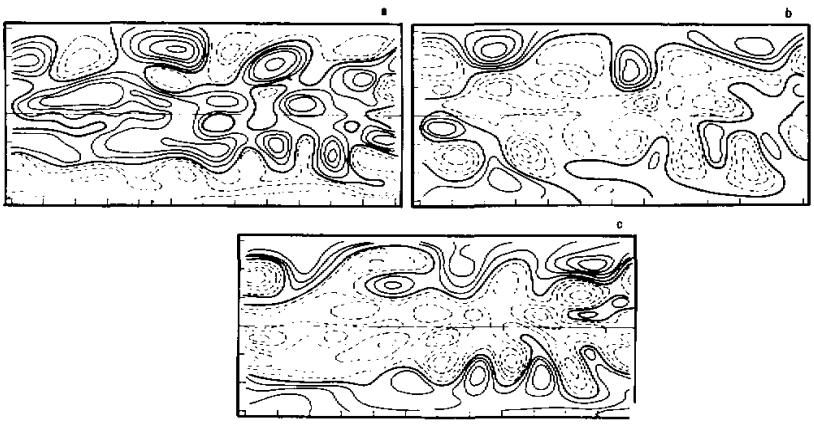

Fig.2. Single–point correlations of 300 hPa geopotential heights in the Northern winter. Interval: 0.20. a) the basic point at 48°N, 112°W; b) the basic point at 56°N, 76°E; c) the basic point at 55°N, 32°W.

and finally, enters the equatorial Pacific; the other originating in the equatorial western Atlantic moves towards the northeast, then turns to the southeast, and goes into the equatorial Indian Ocean in the end. For the northern winter EOF1 continues to strengthen but it becomes weaker in the SH (see Fig.1d). In it there are four alternating positive and negative centres over the North Pacific and North America, whose pattern is analogous to PNA proposed by Wallace and Gutzler (1981), but with the location farther east. There is a pattern of alternating positive and negative centres in the N–S direction similar to a dipole pattern between 30°W and 60°W of the North Atlantic, with its location close to the WA teleconnection. Over the Eurasian continent there is a positive center in Europe, a negative centre in Middle Asia, with a positive–value area in eastern Asia and in the western Pacific, constituting a pattern similar to the EUP teleconnection proposed by Wallace and Gutzler (1981). EOF1 becomes remarkably weak, and its pattern changes greatly as soon as the northern spring comes, and the winter pattern breaks down, with a positive (negative) value area directed zonally at high (mid) latitudes, and again a positive area at tropical and equatorial latitudes. At this time, the SH enters the autumn when EOF1 becomes strong, resulting in a pattern of alternating positive and negative centres originating in the equatorial western Pacific, similar to a wave train.

The above results show the pronounced seasonality in the pattern of the monthly–and seasonal–scale oscillations. The distribution of alternating positive and negative centers analogous to a wave train appears in the winter hemisphere, and especially the NH pattern is similar to teleconnections PNA, WA and EUP of Wallace and Gutzler (1981). Autumn is an important transition season for the pattern, in which the basic characteristics of the winter pattern begin to appear and become increasingly stronger, and finally falls into the winter teleconnection.

To further confirm the results we choose the positive centre (48°N, 112°W) on the EOF1 chart of the NH winter as the basic point to calculate single–point correlations of 300 hPa geopotential heights (Fig.2a). Results show that the pattern is in rough agreement with that of Fig.1d. Also we choose the Asian negative centre (56°N, 70°E) of Fig.2d in the pattern similar to EUP as the basic point to compute single–point correlations (Fig.2b), obtaining a pattern analogous to both that of Fig.2a and Fig.1d; when the basic point is changed to 55°N, 32°W,

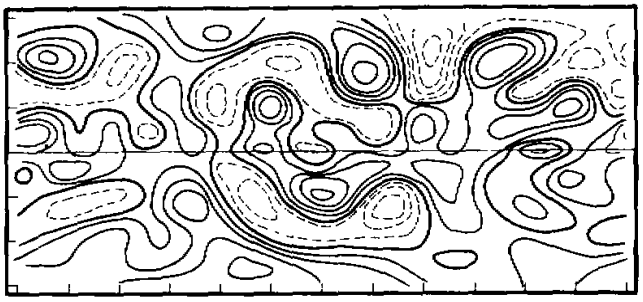

Fig.3. Single-point correlations of 300 hPa geopotential heights in the Northern summer, with the basic point at 47°N, 157°W. Interval: 0.20.

the results remain much the same (Fig.2c). From the analyses one can see that the characteristic distribution of the low-frequency oscillations in the NH 300 hPa geopotential height field really reflects the basic Northern winter features of the model atmosphere. Similar results have been obtained for other seasons. It is worth noting that Fig.3 (the basic point at 47°N, 157°W) for the correlations shows more clearly than in Fig.1b a pattern of alternating positive and negative centres similar to a wave train in the NH summer. It extends from the equatorial western Pacific to the equatorial Atlantic, exhibiting more clearly features of the low-frequency oscillation of the model atmosphere in Northern summer.

IV. INTERANNUAL VARIABILITY OF MONTHLY-SCALE OSCILLATIONS

Fig.4 is the block diagram of time coefficients of EOF1 for 15 winter months, showing a maximum positive coefficient for December of the fifth model year, then for January of the second, and then for February of the first, and a maximum absolute value of the negative coefficient for January of the fifth model year, followed by that for February of the third and December of the second. Monthly averaged 300 hPa geopotential height fields with maximum positive (negative) coefficients of the three months mentioned are synthesized to make a composite field (denoted as M+ (M−), shown in Fig.5a (5b)).

Comparing Figs.5a with 5b, we can see that the pattern of positive-and negative-value

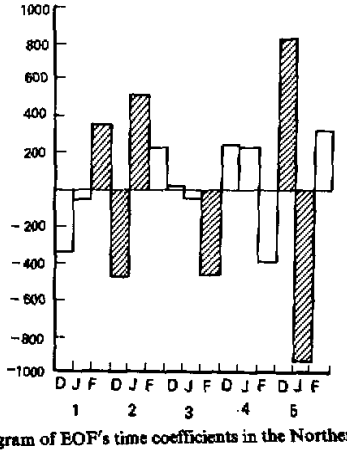

Fig.4. Block diagram of EOF's time coefficients in the Northern winter months.

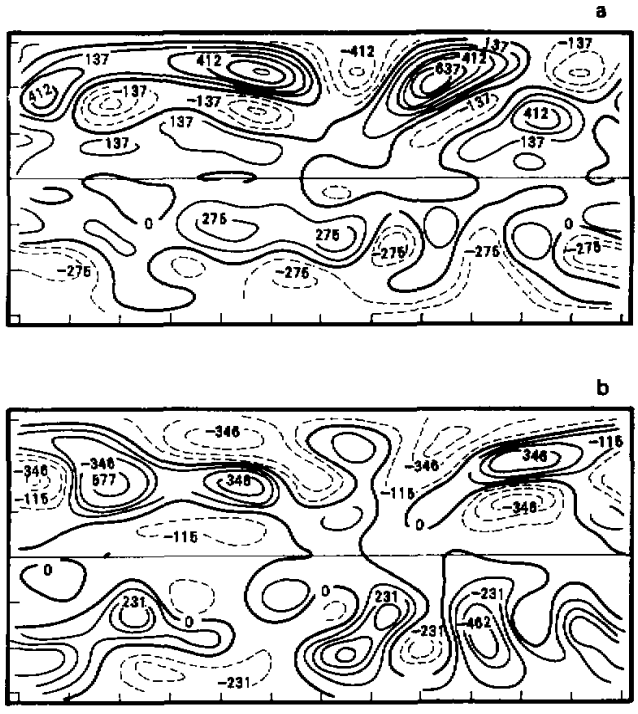

Fig.5. Chart of composite 300 hPa geopotential height in the Northern winter. a) for M+, b) for M−.

areas on the M+ and M− charts is similar, but opposite in sign. This shows clearly that thesituations for M+ and M− reflect adverse climatic states of the winter model atmosphere.

Comparison of Fig.5 with Fig.1d shows that the patterns for M+ and M− are basically similar to those of EOF1 of the Northern winter, with M+ (M−) in agreement with (opposite to) EOF1 in sign. Therefore, the patterns for M+ are those similar to the positive PNA, WA and EUP, and those for M− are the negative patterns.

We draw a field of 300 hPa geopotential height departure for a single month to illustrate further the existence of the interannual variability. Fig.6a(6b) shows the departure field of December (January) of the first (fifth) model year. A teleconnection similar to PNA is seen in Fig.6a with a +, −, +, − sign for the centre analogous to the pattern for M+ over the North Pacific to North America, while there is another teleconnection similar to PNA in Fig.6b, but with a −, +, −, + sign for the centre analogous to the pattern for M−. Fig.7a (7b) shows a departure chart of December (February) of the fifth (second) model year, the former (latter) indicating the pattern of positive (negative) EUP similar to that for M+ (M −).

The results mentioned above illustrate that the anomaly in the model atmosphere can take place without non−seasonal external forcing. It is apparent that this anomaly results from dynamic processes inside the atmosphere. The results also show that without non−seasonal external forcing the model atmosphere can exhibit two adverse climatic states, similar in the departure pattern, but opposite in sign. A positive pattern similar to PNA and EUP can appear even in a particular month of an individual year, while in another individual winter month a negative pattern similar to PNA or EUP can occur, indicating that for the same seasonal external forcing, the adverse climatic states can happen.

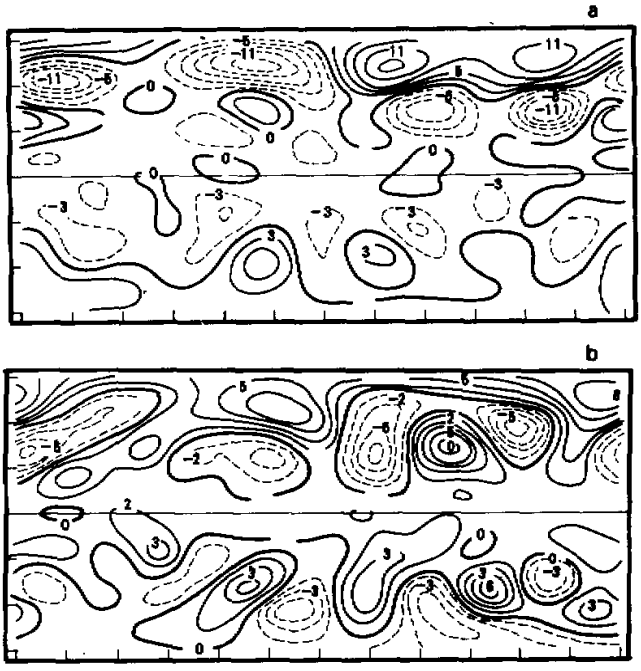

Fig.6. Monthly departure field of 300 hPa geopotential height. Unit: 10m. a) December of the first model year, b) January of the second model year.

V. THE SOURCE FOR THE MONTHLY-SCALE OSCILLATION

The spatial pattern of EOF1 and EOF2 for low-pass filtered 300 hPa velocity potential waves (not shown) shows that their EOF1 and EOf2 are of zonal structure of wavenumber 1, but with a 90° phase difference between.

As we know, components of the wind field found by velocity potential reflect mainly the features of the divergence wind, and the intensity of the tropical divergence wind indicates that of convection. For this reason, analyses of the divergence wind field can lead to understanding the characteristic pattern of tropical convection. Therefore, We make a composite M+ (M−) velocity potential field by the potential with three months of maximum (maximum absolute-value) positive (negative) coefficient of EOF1, and the 300-hPa divergence wind fields thus obtained are illustrated in Figs.8a-b, respectively, to which opposite is the 850-hPa field (figure omitted). As show in Fig.8b, for M− the 850 (300) hPa convergence (divergence) over the tropic Indian Ocean indicates the existence of a strong convective heating region inside the atmosphere (figure for 850 hPa omitted);the lower (upper) divergence (convergence) in the tropic western Pacific indicates the existence of a heat-sink in the atmosphere (figure for 850 hPa omitted); the lower (upper) convergence (divergence) in the midlatitude eastern Atlantic indicates another convective heat source available in the atmosphere, in contrast to the situation over the tropical western Atlantic . Fig.8a depicts the distribution of the convective heat sources and sinks in the tropical atmosphere for M+, with

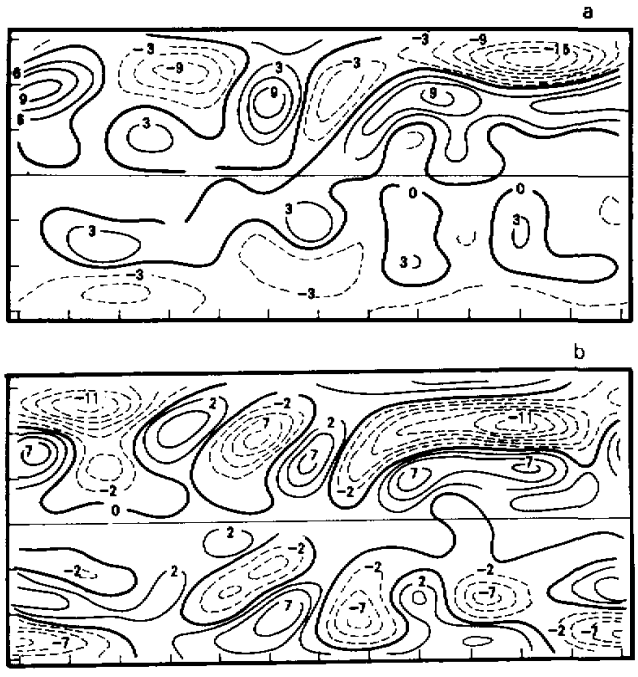

Fig.7. The same as in Fig.6. a) December of the fifth model year, b) February of the second model year

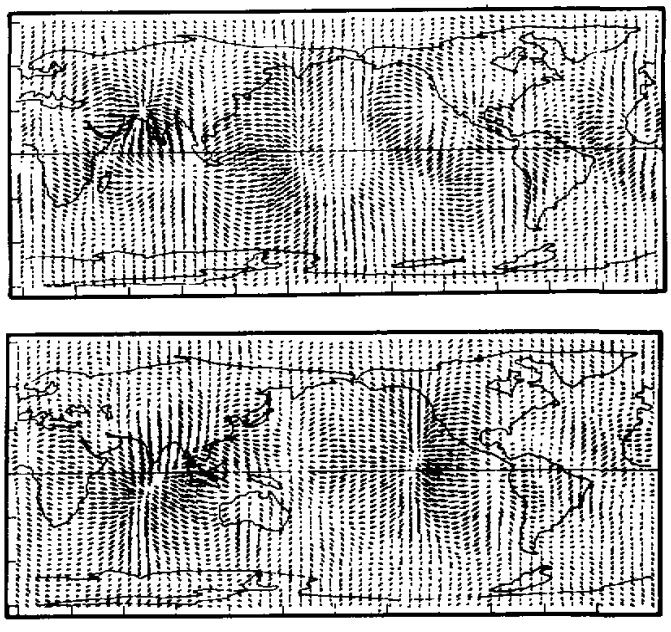

Fig.8. Chart of composite divergence wind field at 300 hPa in the Northern winter. a) for M+; b) for M−

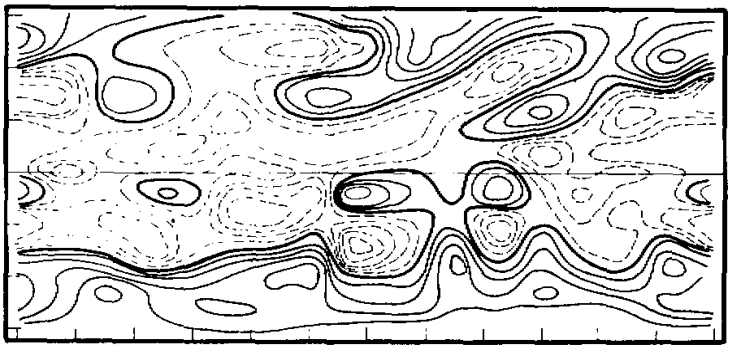

Fig.9. Correlation between averages of 300 hPa velocity potential in an equatorial area and geopotential height in the Northern winter.

features just opposite to those for M−, in which the heat sources are located over the tropic western Atlantic and Pacific, and the sinks are over the midlatitude eastern Atlantic and tropic Indian Ocean. The results show the existence of two different patterns of the tropical heat source and sink for M+ and M−, which is evidently relevant to the two adverse climatic states in the Northern winter. In order to further explain the existence of the relevance we calculate the correlation between the averages of the 300 hPa velocity potential of 7 grid points around the negative centre and 300 hPa geopotential heights of the 15 winter months (see Fig.9). Comparing Fig.9 with Fig.1d and Figs.2a–c one can see that they are not only similar in patterns, but also identical in sign, indicating that the source for the low-frequency oscillation in the model atmosphere remains the convective heat source / sink inside the tropical atmosphere. Comparing Figs.8 with Fig.1d, we find that for M+ the tropic western Pacific and Atlantic serve as the heat source inside the atmosphere, corresponding in the departure pattern to the positive PNA, WA and EUP teleconnection, and for M− the tropic western Pacific and Atlantic serve as the heat sink, corresponding in the departure pattern to the negative PNA, WA and EUP teleconnection. This indicates that the distribution of low-frequency oscillation similar in pattern but opposite in sign for M+ and M− results from the distribution of the heat source / sink similar in pattern but opposite in sign.

VI. DISCUSSION AND CONCLUSION

Analysis is done of seasonal characteristics and interannual variabilities of the monthly-scale low-frequency oscillation by five-year low-pass filtered data from a low-order global spectral model without the non-seasonal external forcing. Results are as follows:

(1) Anomaly can take place inside the model atmosphere without non-seasonal external forcing, a result that agrees with that of Lau (1981), with remarkable seasonal characteristics and interannual variabilities revealed.

(2) Even without non-seasonal external forcing, the model atmosphere can exhibit two adverse climatic states, similar in pattern but opposite in sign as shown in their departure charts, indicating that for the same external forcing the model atmosphere can exhibit two or more climatic states. Obviously, the so-called anomaly is but the manifestation of the adverse states, a result which seems to further support the theory of multi-equilibria proposed by Charney and Devore (1979) in their idealized channel model.

The results also show that for the same external forcing (i.e., without non-seasonal ex-

ternal forcing) some (other) winter months can exhibit the positive (negative) departure pattern similar to PNA, indicating that the model atmosphere itself includes the natural interannual variability of the teleconnection. It can be inferred that with the positive departure pattern similar to PNA due to the variability and with non–seasonal forcing similar to El Nino available the atmospheric climatic state will manifest itself as climatic effect of strengthened El Nino, i.e., the strong positive departure pattern similar to PNA, and *vice versa*, indicating that the influence of the natural variability of the model atmosphere on climatic effect produced in the course of long–term integration should be considered in the numerical study of climatic effect of external forcing or in the short–term dynamic prediction of climatic variation. Therefore, not only does the problem of dynamic prediction of short–range climatic variation concern the initial and boundary values but should be the result from the combined effect of the initial state and natural variabilities of the model atmosphere itself due to the long–term integration with nonseasonal and seasonal external forcing available as well.

(3) The source for the low–frequency oscillation of the global atmosphere remains the convective heat source / sink inside the tropical atmosphere. The anomaly of the tropical heat source / sink affects the global atmosphere through dynamic processes in the atmosphere, resulting in the so–called low–frequency oscillation. Therefore , we should focus our attention to the variation of the convective heat source / sink in the tropical atmosphere in the study of low–frequency oscillation of the global atmosphere. Obviously, it is the key to the exploration of the monthly–scale climatic anomaly.

REFERENCES

Charney, J.G., and J. G Devore (1979), Multiple flow equilibria in the atmosphere and blocking, *J.Atmos, Sci.*, **36**: 1205–1216.

Geisler, J.E., M.L.Blackmon, G.T.Bates and S. Munoz (1985), Sensitivity of January climatic response to the magnitude and position of equatorial Pacific sea surface temperature anomalies, *J. Atmos, Sci.*, **42**, 1037–1049.

Horel, J.O., and J.M.Wallace (1981), Planetary scale atmospheric phenomena associated with the southern oscillation, *Mon. Wea. Rev.*, **109**: 813–829.

Hoskins, B.J., and D.J.Karoly (1981), The steady linear response of a spherical atmosphere to thermal and orographic forcing, *J. Atmos, Sci.*, **38**: 1179–1196.

Lau, N.G. (1981), A diagnostic study of recurrent meteorological anomalies appearing in a 15–year simulation with a GFDL general circulation model, *Mon. Wea. Rev.* **109**: 2287–2311.

Ni Yunqi, Lin Wayin and Ning Dongmei (1990), Numerical study for short– range climatic oscillation forced by El Nino in Northern winter (to be published). *Acta Meteorologica Sinica*, Vol.4, No.5, 554–568.

Shukla, J, and J.M.Wallace, (1983), Numerical simulation of the atmospheric response to equatorial Pacific sea surface temperature anomalies, *J. Atmos, Sci.*, **40**: 1613–1630.

Wallace, J.M., and D.S. Gutzler (1981), Teleconnections in the geopotential height field during the Northern Hemisphere winter, *Mon. Wea., Rev.*, **109**: 784–812.